STRONG FIELD PUMPED NANOWIRE LASER

MARTIN BEYER and MATHIS NOLTE with Daniil Kartashov

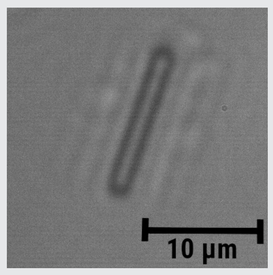

Fig. 1: Image of the nanowire.

Excitation Mechanisms

For nanolasers the excitation mechanisms in the nanowire are important, through which electrons get into an excited energy state. For semiconductor nanowires the relevant mechanisms are multi photon absorption and tunneling ionisation. The predominant mechanism depends on intensity and frequency of the pump light and is indicated by the Keldysh parameter

$$\gamma = \omega \frac{\sqrt{2 m_{\text{eff}} E_g}}{e E_0}$$

[1] which depends on the electric field amplitude E_0 for a given laser frequency ω, bandgap energy E_g, and effective electron mass m_{eff}. For $\gamma \gg 1$ multi photon absorption is the predominant mechanism, while for $\gamma \leq 1$ tunnel ionisation is. The pump laser used in the experiment produced $\tau = 100$ fs (FWHM) long pulses, with a wavelength of $\lambda = 3.85$ µm, a repetition rate of $f_{\text{rep}} = 1$ kHz and a beam radius of $w = 40$ µm. Assuming a peak intensity of 1.5×10^{11} W cm^{-2}, a bandgap energy of 2.32 eV and an effective mass of $0,11 m_e$ [2], the dominant excitation process is tunnel-ionisation with $\gamma = 0.73$.

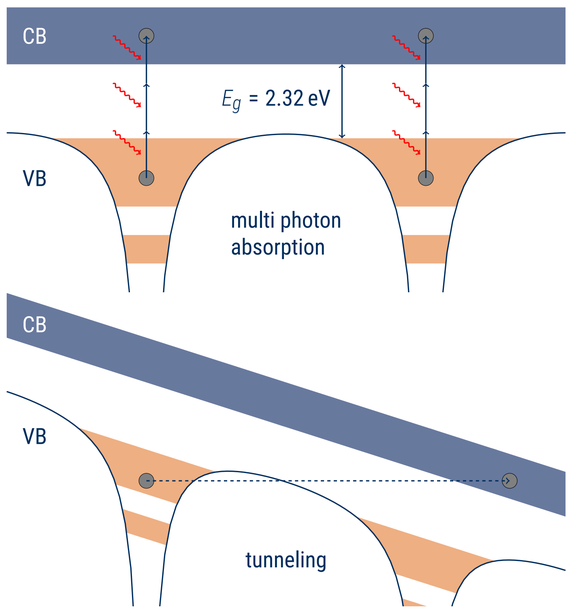

Fig. 2: The two excitation mechanisms.

Polarisation Dependence

The intensity of laser emission is strongly dependent on the polarisation of the pump light. It induces polarisation charges on the surface of the nanowire, which oppose the electric field of the pump light and laser light of the nanowire. Because of the nearly 1D geometry of the nanowire this reduction is dependent on the angle θ between wire axis and polarisation, i. e. for a nearly homogeneous refractive index n the perpendicular component gets reduced by $E_{\text{In},\perp} = \frac{2E_{0,\perp}}{1+n^2}$ (c. f. dielectric cylinder in homogeneous electric field), whereas the parallel component is unchanged $E_{\text{In},\parallel} = E_{0,\parallel}$. The intensity I_{in} is then

$$I_{\text{in}} = \left[\sin^2(\theta) \cdot \left(\frac{2}{1+n^2} \right)^2 + \cos^2(\theta) \right] I_0,$$

where I_{In}/I_0 is the intensity inside/outside the wire. Since the pump light is normal incident on the wire surface, polarisation direction changes due to refraction can be neglected. The absorption efficiency can still depend on the polarisation inside the wire.

The lasing process

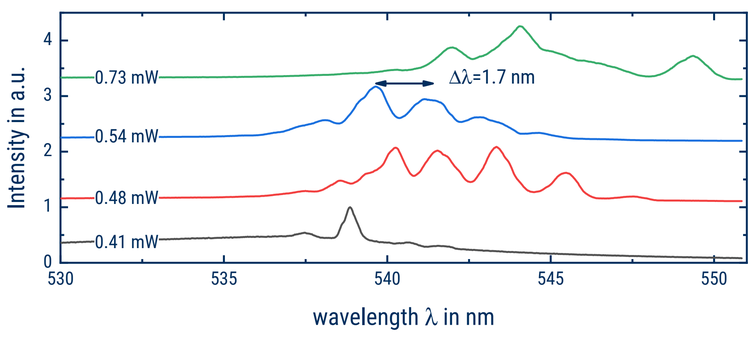

Fig. 3: Spectrum of lasing for parallel orientation and different powers.

It is essential to distinguish between luminescence and lasing. The spectrum of the output intensity develops sharp emission lines for the Fabry-Pérot modes on top of the amplified spontaneous emission. The size of a nanowire can be estimated by projecting an image of the nanowire on a CCD-camera (fig 1) and comparing it to a reference image. The nanowire in the experiment is about 11 µm long. Using the formula [3]

$$\Delta\lambda = \frac{1}{L} \left[\frac{\lambda^2}{2} \left(n - \lambda \frac{\mathrm{d}n}{\mathrm{d}\lambda} \right)^{-1} \right]$$

the group velocity index $\left(n - \lambda \frac{\mathrm{d}n}{\mathrm{d}\lambda} \right)$ can be calculated, which is the ratio of the speed of light in vacuum to the group velocity in a medium. For a mode distance of $\Delta\lambda = 1.7$ nm and $\lambda = 540$ nm the group velocity index is 7.8.

Since the refractive index is a function of carrier density, it also depends on pulse energy. For higher pulse energies (intensities) the Fabry-Pérot modes start smoothing out. This is due to the strong changes in the refractive index over the period of a single pulse. It also leads to a strong change in the mode distances, thus, for a given wavelength in the spectrogram only the temporal integral is visible.

Experimental Setup

The goal of the experiment was to examine the influence of the polarisation direction of the linear polarised pump light on the laser light of a perovskite ($CsPbBr_3$) nanowire. The setup is displayed in fig. 4. The sample is a 500 µm thick sapphire substrate on which nanowires were synthesised via a drop-cast method. A half wave plate in front of the sample was rotated around the beam axis to achieve a tuneable polarisation angle relative to the wire. Since the focal spot of 80 µm could cover several wires, an imaging system including a pin hole was used to select a single nanowire. Behind the imaging system a second polariser was installed, which allowed the analysis of the polarisation state of the output light. The beam was finally fed into a spectrometer or a camera via a beamsplitter on a flip mount.

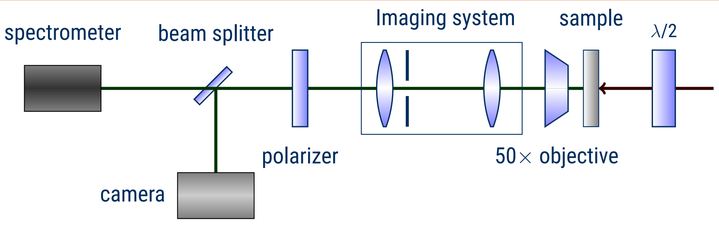

Fig. 4: Experimental setup.

Power and polarisation dependence of lasing

The spectrogram is symmetric about the wire axis which is located at −5° in the spectogram (fig. 5) corresponding to a rotation angle of 10° via the half wave plate. However, measurements in fig. 1 show that the relative angle to the vertical axis is 18.5°. Since a rotation of 180° corresponds to the same wire geometry, the spectrogram shows a two-fold symmetry in the dependence on the polarisation angle. The visible Fabry-Pérot modes exhibit a shift in wavelength for different polarisation angles. A possible explanation is the occurrence of higher transversal modes with different wavelengths. The number of supported modes by the nanowire depends on its diameter d, core n_1 and cladding n_0 refractive index. For single mode lasing, fibers must fulfil the condition [5]

$$V = \frac{\pi}{\lambda_0} d \sqrt{(n_1^2 - n_0^2)} < 2.405.$$

With an estimated refractive index $n_1 = 2.01$ [4] and a diameter $d = 0.5 \ldots 1.6$ µm of the wire, the parameter is $V = 5.03 \ldots 16.1$ which indicates multi-mode lasing. The gain profile behaves asymmetric for increased pump power. For longitudinal modes with higher/lower wavelengths the gain increases/decreases with power. This effect is especially pronounced for a polarisation parallel to the wire.

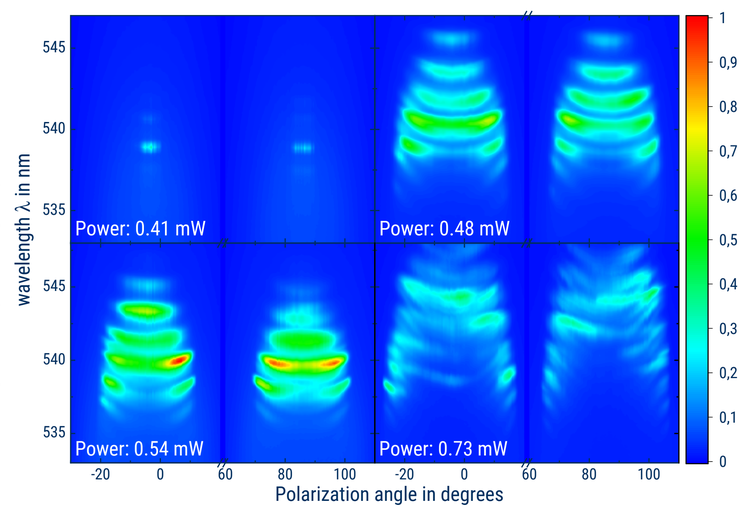

Fig. 5: Spectrogram of lasing for different pump powers which are related to intensity via $I_0 = 1.88P/(\tau\pi w^2 f_{\text{rep}})$.

Polarisation angle resolved measurement of the laser emission

With the polariser behind the nanowire it was possible to analyse laser emission of a single polarisation state. Thus, ten measurements with angles 0° . . . 90° were carried out. Three of them are shown in fig. 6. This setup only made it possible to measure differently polarised components of the light, so linear polarised light could not be distinguished from elliptical polarised light.

In contrast to fig. 5 no shift in the wavelength for a single mode can be observed. and also the summation over all ten polarisation angles differs from the spectrogram (for $P = 0.54$ mW) in fig. 5. It is suspected that the wire was damaged when the pump power was increased to 0.924 mW in the previous part of the experiment, which is larger than two times the lasing threshold.

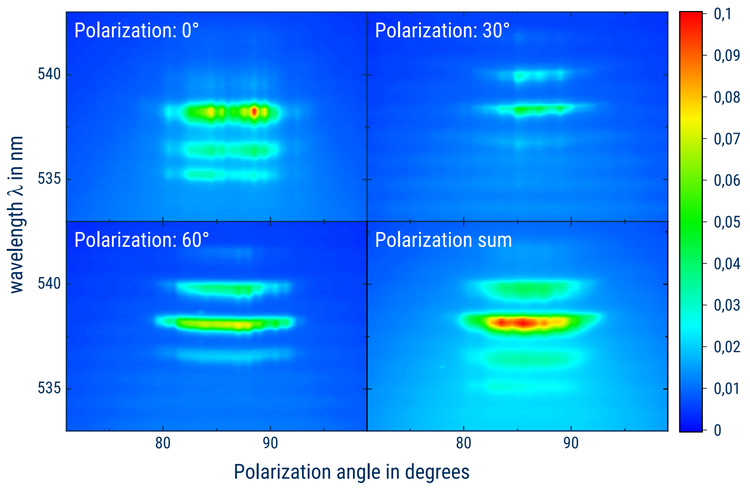

Fig. 6: Polarisation resolved spectrogram of lasing. $P = 0.56$ mW. Bottom right: Sum of 10 measurements with 0° . . . 90°.

Conclusion

The analysis of different pump powers shows, that the lasing of the nanowire exhibits Fabry-Pérot modes which enable the determination of the group index of the material. For different polarisation angles the longitudinal modes exhibit a wavelength shift which may be explained by higher transversal modes. For different pump powers the refractive index changes which leads to a shift towards higher wavelengths for all modes. Furthermore the gain profile shows an asymmetric behaviour for different pump powers. The polarisation angle resolved measurement shows that the nanowire was damaged at pump powers higher than two times the laser threshold.

References:

[1] A. M. Zheltikov, Keldysh photoionization theory: through the barriers, IOP Publishing, 2017
[2] Z. Yang et al., Impact of the Halide Cage on the Electronic Properties of Fully Inorganic Cesium Lead Halide Perovskites, ACS Energy Letters, 2017
[3] M. A. Zimmler et al., Optically pumped Nanowire Lasers: Invited Review, IOP Publishing
[4] W. Yan et al., Determination of complex optical constants and photovoltaic device design of all-inorganic CsPbBr3 perovskite thin films, Optics Express, 2020
[5] G. P. Agrawal, Nonlinear Fiber Optics, Elsevier, 2007

FRIEDRICH-SCHILLER-
UNIVERSITÄT
JENA